



**Universidad de Concepción**  
**Dirección de Postgrado**  
**Facultad De Ingeniería – Programa de Magister en Ciencias de la Ingeniería,**  
**Mención Ingeniería Civil**

**EVALUATION OF PERCRYSTALLIZATION FOR ZERO LIQUID  
DISCHARGE IN THE PULP INDUSTRY**

**(EVALUACIÓN DE PERCRISTALIZACIÓN PARA CERO  
DESCARGA LÍQUIDA EN LA INDUSTRIA DE LA CELULOSA)**



POR

**JUAN JOSÉ MOLTEDO ORTEGA**

Tesis presentada a la Facultad de Ingeniería Civil de la Universidad de  
Concepción para optar al grado académico de Magíster en Ciencias de la  
Ingeniería con mención en Ingeniería Civil

Profesor Guía  
Alex Schwarz

agosto 2021  
Concepción, Chile

© 2021 Juan José Moltedo Ortega

Se autoriza la reproducción total o parcial, con fines académicos, por cualquier medio o procedimiento, incluyendo la cita bibliográfica del documento.



## ACKNOWLEDGEMENTS

This project was funded by Bioforest S.A., Research Institute from ARAUCO. My sincere thanks for allowing the publication of these results.

I thank the Universidad de Concepción for the scholarship granted to the master's degree.

I would like to thank God for all the opportunities that He has provided to develop this program.



Special thanks to Professor Alex Schwarz from Universidad de Concepción and Alvaro Gonzales from Bioforest, for the help and guidance provided.

I would like to thank my family and friend for their constant support.

Finally, people from Bioforest, Jhonny Rossy and Lisette Novoa, together with Wladimir Clavet from Mecfin Ltda. for the help during the experiments.

## ABSTRACT

Percrystallization was evaluated at laboratory scale to determine the suitability of the technique as the core evaporation technology for achieving Zero Liquid Discharge (ZLD) of a Kraft pulping effluent. Compared with conventional evaporation/crystallization, percrystallization allows to operate at room temperature, using relatively inexpensive membranes and vacuum to allow evaporation of aqueous brine solutions. This suggests that it could be an efficient alternative to evaporate the concentrated brine from an upstream desalination stage (electrodialysis), as less energy would be required to heat the solution and allow evaporation. Percrystallization of electrodialysis brine was successfully achieved at laboratory scale, but high energy consumptions over 3,000 kWh/ton were measured. After this, the energy consumption of an optimized industrial system (with an efficient vacuum pump) was computed based on theoretical equations, indicating energy consumptions between 110-150 kWh/ton, still higher than those of traditional ZLD systems based on brine crystallizers (around 90 kWh/ton). Percrystallization could be an efficient alternative for low scale applications where the temperature of the solution must remain low (e.g., less than 40°C).

## CONTENTS

Chapter 1:	Introduction .....	1
1.1	Motivation .....	1
1.2	Hypothesis .....	4
1.3	Objectives .....	4
1.3.1	General objective.....	4
1.3.2	Specific objectives.....	5
1.4	Methodology .....	5
1.5	Structure of the thesis .....	6
Chapter 2:	State of the art review.....	7
2.1	Conventional ZLD systems .....	7
2.2	Novel technologies to increase water recovery .....	10
2.3	New ZLD systems based on membrane technologies.....	12
Chapter 3:	Matherials and methods.....	15
3.1	Computational fluid dynamics model .....	15
3.2	Chemicals and tested solutions.....	20
3.3	Analytical techniques .....	21
3.4	Process and experimental setup.....	22

3.5	Percrystallization performance.....	24
3.6	Theoretical energy consumption .....	25
Chapter 4:	Results .....	31
4.1	CFD Model.....	31
4.2	Obtention and characterization of the industrial ED concentrate.....	33
4.3	Percrystallization performance.....	35
4.4	Energy consumption of an industrial percrystallization system.....	41
Chapter 5:	Conclusions .....	46
References	.....	48



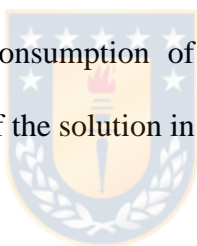
## LIST OF TABLES

Table 3.1. Boundaries and its associated conditions for each physics module.....	19
Table 3.2. Operational conditions of percrystallization tests.....	24
Table 4.1. Characterization of the Kraft pulping effluent and the concentrate from ED after treatment of the effluent.....	34
Table 4.2. Results of percrystallization experiments.....	37



## LIST OF FIGURES

Figure 3.1. Schematic representation of the membrane modelled with COMSOL. ....	17
Figure 3.2. Proposed percrystallization process and laboratory setup. ....	22
Figure 4.1. Fitting of the CFD model to the data reported in the literature. ....	31
Figure 4.2. Pictures of percrystallization membranes. ....	35
Figure 4.3. Diffractogram of the crystals sample obtained after percrystallization of the ED concentrate .....	41
Figure 4.4. Specific energy consumption of an industrial percrystallization system depending on the temperature of the solution in the lumen of the membranes. ....	43





## CHAPTER 1: INTRODUCTION

### 1.1 Motivation

Scarcity of water resources and growing environmental awareness are putting high pressure on the industrial sector all around the globe, especially for industries with high water consumption. Zero Liquid Discharge (ZLD) is a strategy that eliminates liquid wastes, diminishing water consumption and preventing environmental impacts on water bodies. However, ZLD is usually avoided due to its high costs and intensive energy consumption (Yaqub & Lee, 2019). Traditional ZLD systems rely on thermal processes such as evaporators/concentrators and crystallizers, which evaporate water and crystallize the ions present in the effluent, capturing the distillate for further reuse. However, these systems have high energy consumptions, around 39 kWh/ton and 52 kWh/ton of feed water, respectively (Mickley, 2008), becoming an expensive solution. In some cases, they have an even bigger environmental impact in terms of greenhouse gases emissions, as large amounts of these may be released during the production of the required energy, depending on its source (Tong & Elimelech, 2016).

Great efforts have been made to reduce the costs associated with ZLD systems. Combination of well-known desalination processes such as electrodialysis (ED) or reverse osmosis (RO) with evaporators and crystallizers has decreased the overall costs of ZLD systems, as the actual ZLD equipment (evaporators and crystallizers) must only deal with the concentrated reject fraction of the upstream desalination technology, also called the brine (Nayar, Fernandes, McGovern, Al-Anzi, & Lienhard, 2019; Oren et al., 2010). Likewise, the development of novel membrane technologies to further reduce the brine volume prior to the crystallization step has shown promising results (Chabanon, Mangin, & Charcosset, 2016; Drioli, Di Profio, & Curcio, 2012; Yaqub & Lee, 2019). Nevertheless, there are still some problems with these new technologies, such as membrane wetting, concentration or temperature polarization, and fouling and scaling of membranes, the latter being the most detrimental (Ruiz Salmón & Luis, 2018). Moreover, most of these processes cannot achieve crystallization in one step, meaning that they still need an expensive crystallizer to achieve ZLD or filtration of the solution to remove crystals (Pramanik, Thangavadivel, Shu, & Jegatheesan, 2016). These problems appear to have been overcome with a technique called percrystallization (Motuzas et al.,

2018). In this technique, a single step separation of salts and water is achieved thanks to the use of carbonized sucrose hydrophobic membranes (contact angle  $\sim 107^\circ$ ), which allow continuous crystallization on the permeate side of the membranes. This side is exposed to vacuum (around 18 mbar absolute pressure), enabling both low temperature water evaporation and ejection of the crystals formed under supersaturation conditions. Since the salts crystallize on the permeate side, fouling and scaling are prevented on the feed side.

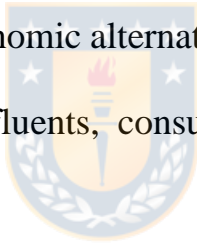


To this date, previous research with percrystallization has been focused on the production of pure crystals (Madsen, Motuzas, Julbe, Vaughan, & Diniz da Costa, 2019; Madsen, Motuzas, Vaughan, Julbe, & Diniz da Costa, 2018; Motuzas et al., 2018) rather than water recovery for ZLD systems. Therefore, no experiments on multiple salts solutions have been made so far. This is crucial for ZLD, since most industrial effluents have multiple ions which form different type of crystals and their interaction in percrystallization must be studied. Moreover, there are no reports on the energy efficiency or investment costs for percrystallization, mostly because it is still at laboratory scale. Considering that it allows evaporation at low temperatures, it could be

a more economic and energy efficient way to achieve ZLD compared with traditional crystallizers. Therefore, this work evaluates the capacity of percrystallization to evaporate the brine from an ED treated Kraft pulp mill effluent and compares the efficiency of the process with traditional ZLD systems.

## **1.2 Hypothesis**

Percrystallization is an economic alternative to achieve zero liquid discharge of industrial pulp mill effluents, consuming less energy than traditional evaporation systems.



## **1.3 Objectives**

### **1.3.1 General objective**

Evaluate the use of percrystallization for zero liquid discharge systems of industrial pulp mill effluents, in terms of effectiveness and energy consumption.

### 1.3.2 Specific objectives

- Evaluate the technical capacity of percrystallization at laboratory scale to treat the concentrated reject (brine) from an electro dialysis system and achieve zero liquid discharge.
- Compare percrystallization with traditional zero liquid discharge systems in terms of energy consumption.

### 1.4 Methodology



Percrystallization experiments were performed at laboratory scale, with synthetic simple and binary salt solutions, and with real industrial effluent from a Kraft pulp mill, which was previously concentrated by electro dialysis. General performance was evaluated, along with energy consumption and solution fluxes. Additionally, a simple computational fluid dynamics model was used to identify the main parameters of the process. Finally, the energy consumption of an industrial size percrystallization system was computed using theoretical equations.

## 1.5 Structure of the thesis

Chapter 1 presents the studied problem, including the motivation for the work, hypothesis, objectives, and a brief description of the methodology.

Chapter 2 introduces the reader to the state of the art of zero liquid discharge systems, explaining the different lines of studies that have been developed.

Then, the methodology of this research is described in Chapter 3, focusing on materials and methods employed. Chapter 4 presents the main results of

this study and a brief discussion. Finally, Chapter 5 gives the conclusions of this work.



## CHAPTER 2: STATE OF THE ART REVIEW

### 2.1 Conventional ZLD systems

Early ZLD systems relied on thermal processes alone to evaporate wastewater, first in brine concentrators and then in brine crystallizers or evaporation ponds, recovering the condensed distillate for reuse and disposing the produced solids in landfills or selling them as valuable byproducts (Tong & Elimelech, 2016). This traditional scheme was even implemented in a bleached chemithermomechanical pulp mill in Canada, using mechanical vapor recompression (MVR) evaporators and steam driven concentrators (Evans, 1995). Nowadays, desalination techniques have been incorporated into ZLD processes to minimize the costs of the systems. These technologies, such as reverse osmosis (RO), are usually employed in seawater desalination facilities, where freshwater is produced together with a concentrated brine, which comprises less than 50% of the feed volume and is typically discharged back into the sea (Elimelech & Phillip, 2011). The incorporation of an economic and less energy demanding desalination stage prior to the actual ZLD system (mainly brine concentrators and crystallizers) reduces the amount of water to be evaporated, diminishing both operational

and capital expenditures (Yaqub & Lee, 2019). The selection of the most appropriate desalination technology depends on the application. Reverse osmosis is a pressure driven technology, primarily used for seawater desalination. The solution flows through a semipermeable membrane that rejects ions and allows passage of water, producing water with very good quality (Elimelech & Phillip, 2011). However, it requires rigorous pretreatment, as it is prone to fouling due to the direction of the permeate flow, perpendicular to the membranes. On the other hand, electrodialysis is a desalination technique that relies on an electric field to promote the transfer of ions through cation and anion exchange membranes. The electric field is generated by the potential difference between a cathode and an anode, which attract cations and anions, respectively (Klein, Ward, & Lacey, 1987). Considering the direction of the liquid flow, parallel to the membranes, it has a higher resistance to fouling and requires less rigorous pretreatment than RO, so it may be a better option for ZLD applications in some industrial effluents with high organics or suspended solids content (Chen, Ren, Tian, Sun, & Wang, 2019; Gonzalez-Vogel, Moltedo, Reyes, Schwarz, & Rojas, 2021). Additionally, it produces a lower volume of reject brine (concentrate)



compared with RO, which directly reduces the size and cost of the evaporation stage (Havelka, Farova, Jiricek, Kotala, & Kroupa, 2019).

Great efforts have been made to maximize the water recovery of the desalination stages. Heijman, Guo, Li, van Dijk, and Wessels (2009) studied the removal of scaling components (calcium, magnesium, barium and silicate) before entering a nanofiltration stage (another membrane desalination technique, similar to RO), achieving 99% recovery in groundwater desalination. Brine minimization with electrodialysis reversal (EDR) was evaluated by D. Zhao et al. (2019), reducing the volume of the concentrate reject from a RO treatment of a petrochemical industry effluent by 6.5 times. These strategies aim to achieve an affordable ZLD system, but they fall short in reducing the costs and energy consumptions of evaporator/crystallizers. Even in an optimized zero brine discharge seawater desalination system, which hybridizes RO with electrodialysis to achieve nearly 82% recovery prior to the crystallization stage (technically limited), one third of the specific water cost comes from the crystallization subsystem (Nayar et al., 2019).

## 2.2 Novel technologies to increase water recovery

Considering the high costs of current evaporation systems for ZLD, in recent years researchers have shifted their efforts towards new membrane technologies that may be a more efficient alternative than existing evaporators or brine concentrators, typically mechanical vapor compressors (MVCs). One alternative is forward osmosis (FO), which extracts water from the feed solution to a concentrated draw solution due to osmotic pressure difference. The solutions are separated by a semipermeable membrane, that allows passage of pure water molecules, rejecting the solute (Valladares Linares et al., 2014). The feed solution leaves the system with a lower water content (higher concentration) and may be directed to a brine crystallizer for ZLD purposes. On the other hand, the draw solution is regenerated by means of a distillation column, as it consists of thermolytic ionic solutes (mainly  $\text{NH}_3/\text{CO}_2$ ) that evaporate when the solution is heated, leaving almost pure water behind (McGinnis, Hancock, Nowosielski-Slepowron, & McGurgan, 2013). By including FO into a ZLD system, the size and energy demand of the brine crystallizers is reduced. This approach was used at the Changxing power plant in China, achieving ZLD of  $650 \text{ m}^3/\text{d}$  of wastewater by

combining FO with a crystallizer to treat the brine from the main RO desalination system (Oasys Water, 2017).

Another technology that aims to increase the recovery of RO or EDR beyond their salinity limit is membrane distillation (MD). This technology uses low grade thermal energy (waste heat) to concentrate brine solutions up to almost saturation, aided by hydrophobic microporous membrane. These membranes only permit the flux of vapor, driven by the temperature difference between the feed and permeate side, that creates a vapor pressure difference. It is an energy intensive process since it requires the liquid phase of the solution to transition into gas phase, but it has the advantage that it can use low grade thermal energy to drive the process. However, there are currently no reported large-scale applications of MD, just laboratory or small-scale pilot tests (Yaqub & Lee, 2019). Moreover, both membrane distillation and forward osmosis do not allow to achieve ZLD without a posterior brine crystallizer but do help to reduce the costs of this last stage.

### 2.3 New ZLD systems based on membrane technologies

Brine minimization prior to the crystallization stage has reached a plateau and researchers are focusing on strategies for specific wastewaters. However, there is still room to create new technologies that may replace brine crystallizers, which are the industry gold standard and point of comparison.

In the past years, membrane distillation above saturation limits, also called membrane crystallization (MCr) has been studied. It shows better control of the nucleation and growth of the produced crystals, thanks to the uniform evaporation rate through the membranes. Thus, it produces better quality crystals compared with conventional crystallizers. However, low fluxes are reported, all below 6 kg/m<sup>2</sup>/h. Additionally, fouling problems may occur if the operational conditions are not selected accordingly (Ali, Quist-Jensen, Macedonio, & Drioli, 2015).

Recently, the development of percrystallization as a new crystallization approach appears to have solved most of the technical issues that are present in MCr. In this technology, the concentration of the circulating solution (from

the feed tank) remains constant, avoiding scaling and fouling. The solution flows through the lumen of carbonized sucrose hydrophobic membranes and a fraction permeates across the membranes, driven by the pressure difference generated by the vacuum on the permeate side of the membranes. Both solute (salts) and solvent (water) pass through the pores of the membranes and form a thin film on the permeate side. As water evaporates on this thin film and is extracted (as vapor) from the vacuum chamber by a vacuum pump, crystals grow and fall due to gravity. If any scale is produced, it is on the outer side of the membrane, as the concentration on the feed side remains stable. Two more advantages of this technique are that evaporation at low temperatures is possible (given that vacuum pressure is below water vapor pressure), minimizing the energy required to heat the solution, and that salts are separated from water in a single step, producing only dry crystals and vapor, which is later condensed on a cold trap.

Permeation may be confused with vacuum membrane distillation (VMD), as both processes employ hydrophobic membranes and vacuum. However, VMD is a concentration process which extracts liquid from the target solution by means of a vapor flux through the membranes (Pramanik

et al., 2016). In percrystallization, both liquid and solids flow across the membrane, without changing the concentration of the feed solution.

Effluents from Kraft mills have total dissolved solids (TDS) in the order of 1000 to 2000 mg/L (Gonzalez-Vogel et al., 2021) and may be characterized as brackish water. Therefore, the use of percrystallization to achieve ZLD in this application must be coupled with an upstream desalination stage, both to minimize the overall costs of the process and to achieve a TDS concentration closer to the saturation point, taking into account that previous experiments have been carried out at concentrations above 125 g/L (Motuzas et al., 2018). Considering the characteristics of ED, it appears to be the best available option to concentrate the Kraft effluent. The concentrate, less than 10% of the treated wastewater, could be sent to a percrystallization system instead of traditional MVCs based brine crystallizers.

## CHAPTER 3: MATERIALS AND METHODS

### 3.1 Computational fluid dynamics model

The CFD model was developed with the software COMSOL Multiphysics (COMSOL, 2005), due to its capacity to couple the different physics phenomena required to explain the percrystallization process, such as liquid flow, permeation through porous media, and heat exchange. The CFD model was adjusted to the available literature data sets (Madsen et al., 2019; Madsen et al., 2018; Motuzas et al., 2018) and its results were used to further understand the technique and identify the most relevant parameters.

Percrystallization may be explained by two main processes: the permeation of the solution through the membrane, driven by the pressure gradient caused by the vacuum, and the evaporation process in the thin film formed on the permeate side. Research on this second process requires complex models (Plawsky et al., 2014; Ranjan, Murthy, & Garimella, 2011; Xiao, Maroo, & Wang, 2013; J.-J. Zhao, Duan, Wang, & Wang, 2011) and is out of the scope of this work, but it can be assumed that it occurs as long as the vapor pressure of the solution is higher than the vacuum pressure of the chamber. On the

contrary, the flux through the membrane can be easily represented by Darcy's law, shown in Equation 3.1.

$$u = -\frac{k}{\mu} \nabla p \quad (3.1)$$

Where  $u$  is the Darcy velocity (m/s),  $k$  is the permeability of the porous medium ( $\text{m}^2$ ),  $\mu$  denotes the dynamic viscosity of the fluid ( $\text{kg m}^{-1} \text{s}^{-1}$ ), and  $p$  is the pressure (Pa). Velocity  $u$  is directly related to the water flux through the membrane.



The steady state model considers Darcy's law as the main equation to solve, which is easy to apply if all terms are known; however, the viscosity of the solution depends on the temperature and concentration of the solution (Ozbek, 1977). Thus, the temperature in every point of the model must be known to properly solve Darcy's law. The effect of concentration was neglected, as the term  $k/(\alpha \mu)$ , where  $\alpha$  is the modification factor due to salinity, may be mathematically rewritten as  $k_m/(\mu)$ , where  $k_m$  is a modified permeability. Therefore, when optimizing the model to find the permeability



$k$  that better fits the experimental data (based on minimization of the medium absolute error of the predicted fluxes),  $k_m$  will be found and, indirectly,  $\alpha$ . Darcy's law and heat transfer (for the temperature) can be implemented with interfaces or modules provided by COMSOL. However, the laminar flow of the solution through the lumen of the membrane must be modeled as well, since it is the only assumed heat source of the system, neglecting the heat transfer with the ambient and the rest of the vacuum chamber. This flow is represented by the Navier-Stokes equations. All these interactions are shown in the representation of the membrane in Figure 3.1.

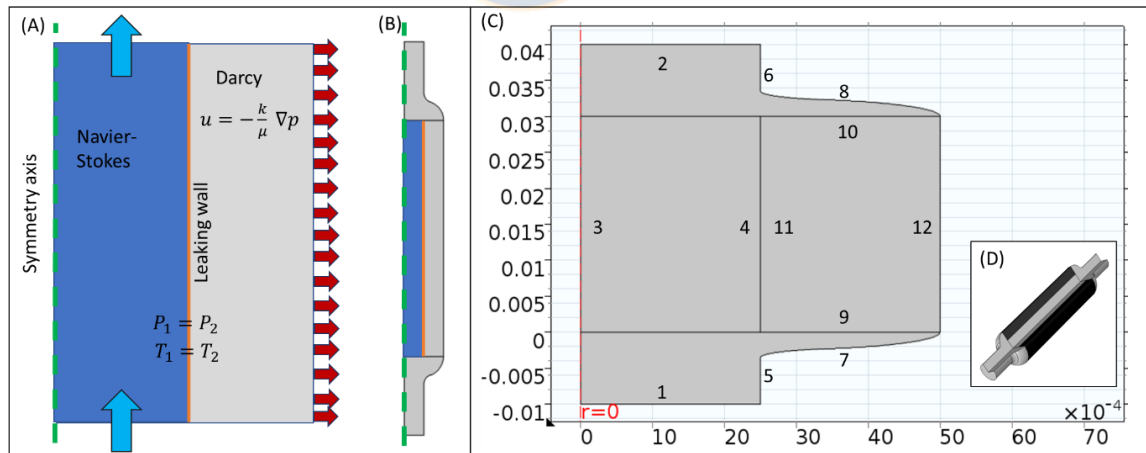


Figure 3.1. Schematic representation of the membrane modelled with COMSOL. (A) Axisymmetric view of the membrane, showing the fluid direction (cyan arrows) and the permeation of the fluid through the pores of the membranes (red arrows); (B) Preserved aspect ratio view; (C) Equal axis view with identified boundaries of the system; (D) 3D cut view of the modelled system. All dimensions are shown in meters.

Given the low fluid velocity and small diameter of the lumen, laminar flow was assumed. Flux through the membrane is promoted by pressure difference between the inner and outer shell of the membrane and has very low velocities, in the order of  $10^{-6}$  m/s. There is a pressure continuity on the inner membrane boundary, which at the same time defines the boundary between the laminar flow and Darcy's law regimes. Pressure on the outside of the membrane is considered equal to the vacuum pressure. Heat is transferred by convection and conduction. The inlet temperature was assumed constant, as the solution is fed from a temperature-controlled tank, being the only heat source assumed for the system. Heat is lost due to evaporation on the permeate side of the membrane. In the model we considered the membrane length and the coupling between the hose and the membrane, simulated as an axisymmetric domain. In steady state models, boundary conditions are relevant to have accurate results. Initial conditions, on the other hand, help the solver reach a solution faster. Therefore, only boundary conditions of the simulation domain are presented in Table 3.1. The identifiers of each boundary correspond to the labels depicted in Figure 3.1 (C).

Table 3.1. Boundaries and its associated conditions for each physics module

Boundary Identifier	COMSOL module		
	Laminar Flow	Darcy Flow	Heat Exchange
1	Inlet	N.A.	Inflow, constant temperature
2	Outlet (1000 Pa relative pressure)	N.A.	Outflow (No restriction)
3	Symmetry axis	N.A.	Symmetry axis
4	Leaking wall	N.A.	Temperature continuity
11	N.A.	Pressure continuity	Temperature continuity
5; 6; 7; 8	No slip wall	N.A.	Thermal insulation
9; 10	No slip wall	No flow border	Temperature continuity
12	N.A.	Constant pressure (vacuum)	Heat flux (loss) due to evaporation

The outlet pressure at boundary 2 is almost atmospheric pressure, as the solution still needs to travel through the hoses that connect the vacuum chamber with the feed tank. Thus, a value of 1.0 kPa (relative pressure) was established. Inlet pressure is determined by COMSOL based on the head losses produced by the walls of the tube (inner side of the membrane) for a given flow velocity. Once the model was set and all boundary conditions were applied, conditions of each experiment were introduced. An initial permeability value  $k$  to begin the adjustment of the model was derived from Equation 3.1, assuming constant temperature.

### 3.2 Chemicals and tested solutions

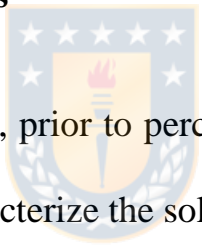
NaCl and Na<sub>2</sub>SO<sub>4</sub> (analytical grade) were obtained from Merck Chemicals. Then, two synthetic solutions were prepared, a 17.5% (w/v) NaCl as a simple salt solution, and 17.5 % NaCl plus 13.5% (w/v) Na<sub>2</sub>SO<sub>4</sub> as a binary salt solution. Sodium sulphate was selected as the second salt because it is the second most important compound in the effluent from the analyzed pulping mill.



The real solution to be percrystallized consisted of the concentrated effluent from a pulping mill. Electrodialysis was selected as the concentration method, given its higher resistance against fouling and the generally higher recovery ratios compared to RO. A commercial ED bench-scale unit was used for obtaining the concentrate (PCCell GmbH, Germany). The equipment included a power supply, pumps, automatic valves, and an electrodialysis cell (ED64). Five pairs of ion exchange membranes (PC-SA anionic and PC-SK cationic, PCCell, Germany) were used, to provide a total surface area of 640 cm<sup>2</sup>. The flow rate was fixed at 20 L/h, with a linear flow velocity of 2.78 cm/s, considering spacers with a thickness of 0.05 cm and a

membrane effective area of 64 cm<sup>2</sup>. The rinsing compartment of electrodes incorporated a 0.25 M Na<sub>2</sub>SO<sub>4</sub> aqueous solution with a flow of 50 L/h. The solutions were kept at 30°C by means of an external water jacket. This ED system was operated in batch mode, where the concentrate was continuously recirculated to a concentrate tank and the diluate to a diluate tank. The experiments were performed until reaching 90% of water recovery.

### 3.3 Analytical techniques



Samples of the concentrate, prior to percrystallization, were analyzed in an external laboratory to characterize the solution in terms of anions (ICS-2100 and Integriom, Dionex), cations (7300 DV and Lambda 25, Perkin Elmer) and other parameters such as pH and conductivity (Seven Multi, Mettler Toledo), chemical oxygen demand (TR320, Merck) and true color (DR 900, Hach). Additionally, a sample of crystals produced by percrystallization was analyzed with X-ray diffraction (Bruker D4 with Lynxeye detector, operated with Cu radiation and K-beta filter, Germany) to identify produced minerals.

### 3.4 Process and experimental setup

Membranes were provided by Dr. Motuzas, University of Queensland, Australia. The experiments were based on previous works (Madsen et al., 2019; Madsen et al., 2018; Motuzas et al., 2018). Figure 3.2 shows the proposed ED-percrystallization system, together with the laboratory setup.

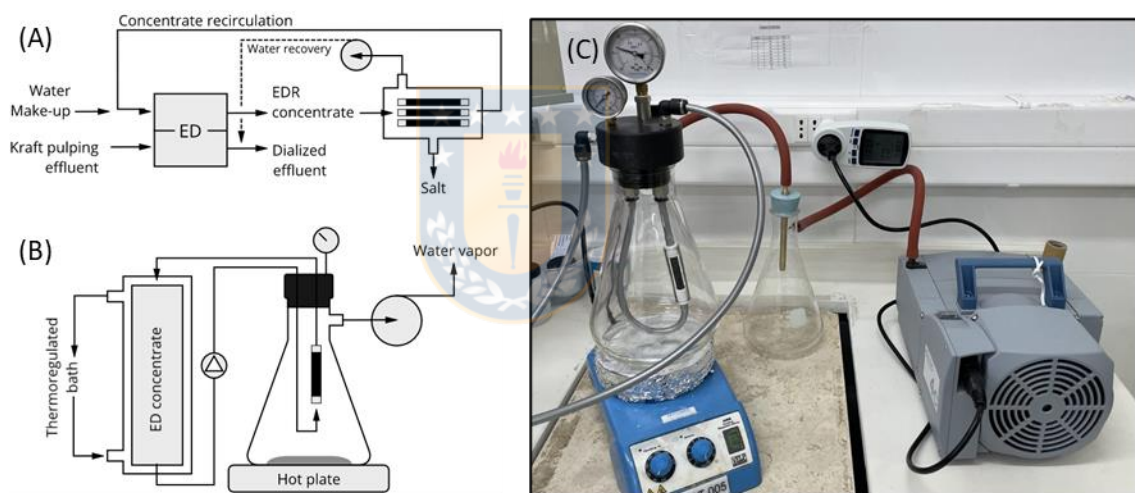


Figure 3.2. Proposed percrystallization process and laboratory setup. (A) Simplified diagram of percrystallization coupled to electro dialysis as ZLD process. (B) Diagram of setup at laboratory scale. (C) Experimental setup to evaluate percrystallization.

The vacuum chamber shown in Figure 3.2 (C) was made of a modified Büchner flask, whose cap allowed the attachment of a vacuum gauge, a vacuum release valve, a manometer, and inlet and outlet connections for the

solution. The preexistent lateral socket of the Büchner flask was connected to the vacuum pump (Vacuubrand, MD 4C NT) with a safety flask in between to protect the pump from any particle (crystals) that could be sucked. Compared with previous works, we did not use a cold trap, since the pump (membrane vacuum pump) could endure operating with water vapor. The vacuum chamber was placed on a hot plate to provide a constant base wall temperature of 50°C. The energy consumption of the vacuum pump was measured with a power meter connected between the pump and the wall socket (Kuman KW47-US).



The concentrated solution (synthetic or ED concentrate) was recirculated through the system by a centrifugal pump with a flow rate of 50 L/h. Water temperature was held constant by a jacket connected to a thermoregulated bath. Evaporated water was computed as the difference between the feed volume before and after percrystallization, measured with a graduated cylinder. Only one hydrophobic membrane was used, whose dimensions were 5 cm length, 9 mm external diameter and 5 mm internal diameter. The effective length was 3.5 cm though, when the area blocked by the connections was subtracted.

### 3.5 Percrystallization performance

The operational conditions of the different percrystallization tests are shown in Table 3.2.

Table 3.2. Operational conditions of percrystallization tests

<b>Purpose</b>	Verification	Base case		Evaluation
<b>Solution</b>	Simple solution	Binary solution 1 (BS1)	Binary solution 2 (BS2)	ED Concentrate
<b>Hot plate</b>	No	Yes	Yes	Yes
<b>Solution temp. (°C)</b>	36.5	38°C	36.5°C	36.5°C
<b>Test time (min)</b>	30	45.5	120	> 90

The purpose of the first test was to verify the performance of the assembled percrystallization setup, using the same conditions and solution (simple NaCl solution) as those used in previous works (Motuzas et al., 2018). Then, experiments with binary salt solution (NaCl/Na<sub>2</sub>SO<sub>4</sub>) were carried out to establish a modified base, in contrast to the single salt solution experiments performed by other authors. Some problems (formation of droplets) were identified during the verification test, so a hot plate under the vacuum chamber was placed and the temperature of the solution was raised, to see if an additional 6 mbar of water vapor pressure could aid in the evaporation



process (BS, Table 3.2). As the test was successful, the temperature was brought back to the starting point (BS2, Table 3.2). After the base case was established, three experiments with the ED concentrate solution were performed.

### **3.6 Theoretical energy consumption**

The main power demanding components of an industrial percrystallization system would be the vacuum pump and the solution heating device. First, a theoretical equation was applied to estimate the energy consumption of the vacuum pumping system, required to maintain the chamber pressure below water vapor pressure of the solution at a defined temperature. The selected formula was used by Miladi, Frikha, and Gabsi (2021) to predict vacuum pump energy consumption of a VMD system, coupled with solar thermal energy to heat the solution. It was developed for a liquid ring vacuum pump (LRVP) that continuously pumps vapor out of the system, keeping the vacuum pressure at the required level, in a similar way to percrystallization. The only difference is that in VMD vapor is produced on the feed side, whereas in this case vapor is produced on the permeate side. It must be noted

that the equation used to compute the power of the LRVP is only a part of the complex model developed to evaluate VMD coupled with solar thermal energy. The power consumption of a LRVP is given by Equation 3.2.

$$\dot{W}_{LRVP} = \frac{P_{in} \dot{V}_{gas} \ln\left(\frac{P_{out}}{P_{in}}\right)}{3.6 * 10^6 \eta_{LRVP}} \quad (3.2)$$

Where  $\dot{W}_{LRVP}$  is the power consumption (kW),  $P_{in}$  is the suction pressure (Pa) or the pressure inside the vacuum chamber,  $P_{out}$  is the discharge or atmospheric pressure (Pa),  $\eta_{LRVP}$  is the efficiency of the pump (0.85 in this case) and  $\dot{V}_{gas}$  is the volumetric flow rate of gas (m<sup>3</sup>/h), which in percrystallization is mostly water vapor.

The vapor produced by the membranes must be equal to the vapor sucked by the vacuum pump, to keep the pressure of the chamber below the saturation pressure of the solution. Therefore, the volumetric flow rate of gas  $\dot{V}_{gas}$  is given by the water mass rate of evaporation and the density of the produced vapor, which depends on the pressure of the system. Assuming that the vapor

is pure gaseous water, the density can be computed by the law of ideal gases, and the vapor flow rate is defined by Equation 3.3 below:

$$\dot{V}_{gas} = \frac{\dot{M}_{conc}}{MW_{H2O}} * \frac{R T_{ch}}{\frac{P_{in}}{101325} * 1000} \quad (3.3)$$

Where  $\dot{M}_{conc}$  is the mass of water to be evaporated (kg/h),  $MW_{H2O}$  is the molecular weight of water (0.018 kg/mol),  $R$  is the universal constant of gases (0.082 atm L mol<sup>-1</sup> K<sup>-1</sup>),  $T_{ch}$  the temperature inside the vacuum chamber (K) and  $P_{in}$  is the pressure inside the chamber (Pa). For simplicity,  $T_{ch}$  was considered equal to the temperature of the solution flowing through the inner side of the membranes, as its difference has a negligible effect on  $\dot{V}_{gas}$  (Equation 3.3).

$P_{in}$  must be lower than the water vapor pressure  $P_{vap}$  of the solution at the defined temperature  $T_{ch}$ . As a precaution, it was defined as 80% of the vapor pressure  $P_{vap}$ . This avoids the need to consider the reduction of vapor pressure produced by the dissolved solids of the solution, which for this case

is in the order of 5%. The simplified formula created by Huang (2018) shown in Equation 3.4 was used for the computation of  $P_{vap}$ .

$$P_{vap} = \frac{\exp\left(34.494 - \frac{4924.99}{T_w + 237.1}\right)}{(T_w + 105)^{1.57}} \quad (3.4)$$

Where  $P_{vap}$  is the water vapor pressure (Pa) and  $T_w$  is the liquid water temperature ( $^{\circ}\text{C}$ ), considered equal to  $T_{ch}$  (K). Thus, considering a safety margin of 80%,  $P_{in}$  is defined as:

$$P_{in} = 0.8 P_{vap} \quad (3.5)$$

On the other hand, the energy required to heat the incoming concentrate up to the defined operational temperature of the percrystallization system was computed based on the temperature difference and the specific heat capacity of water, neglecting its variation with temperature. Additionally, a general efficiency of 0.9 was established, which would change based on the technology. For example, the original model considers that solar energy is directly used to heat the fluid, but it could be replaced with a heat exchanger

(Miladi et al., 2021). Finally, the power consumption of the heating system is defined by Equation 3.6:

$$\dot{W}_{Heat} = \frac{c_w (T_{ch} - T_{con})}{3600 \eta_{Heat}} \dot{M}_{conc} \quad (3.6)$$

Where  $\dot{W}_{Heat}$  is the power consumption (kW) required to heat the concentrate mass flow rate  $\dot{M}_{conc}$  (kg/h) from its original temperature  $T_{con}$  (K) to the temperature of the solution flowing through the percrystallization system  $T_{ch}$  (K).  $c_w$  is the specific heat capacity of water (4.18 kJ/kg/K) and  $\eta_{Heat}$  is the efficiency of the heating system (considered as 0.9). Finally, after normalizing the power consumption by the mass flow rate of the concentrate to be evaporated, the specific energy consumption of the system was obtained, as shown in Equation 3.7.

$$\frac{1000 \dot{W}_{Heat}}{\dot{M}_{conc}} + \frac{1000 \dot{W}_{LRVP}}{\dot{M}_{conc}} = E_{heat} + E_{vacuum} = E_{perc} \quad (3.7)$$

Where  $E_{heat}$ ,  $E_{vacuum}$  and  $E_{perc}$  are the specific energy consumptions (kWh/ton) of the heating, vacuum and complete percrystallization systems, respectively.



## CHAPTER 4: RESULTS

### 4.1 CFD Model

The CFD model was used to replicate the data available in the literature. The fluxes predicted by the model against those reported for different conditions are shown in Figure 4.1.

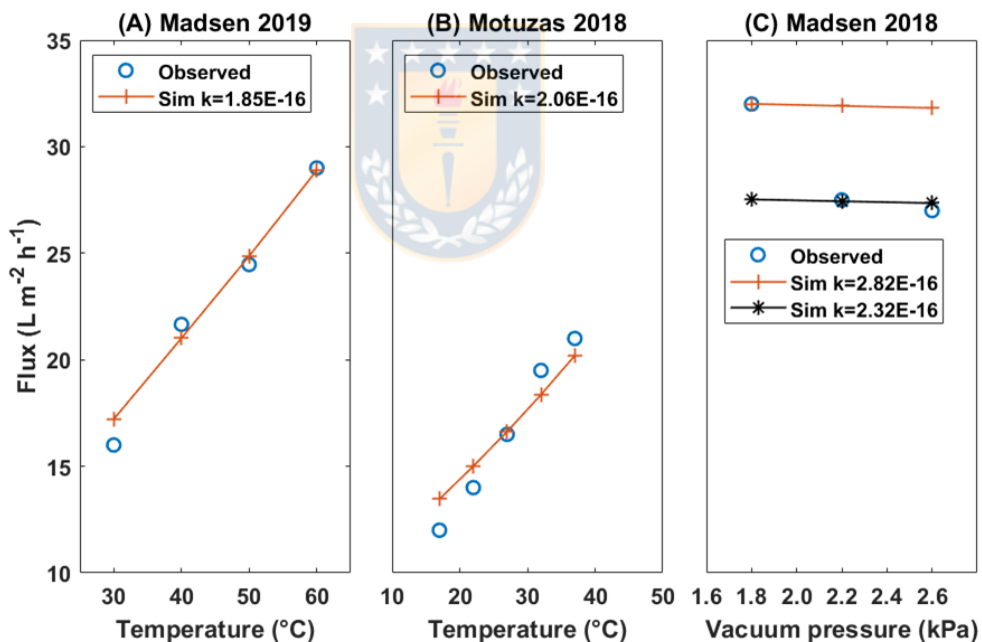


Figure 4.1. Fitting of the CFD model to the data reported in the literature. (A) 40 g/L Ni<sub>2</sub>SO<sub>4</sub> at 2.2 kPa, (B) 125 g/L NaCl at 1 Pa, (C) 175 g/L NaCl at 37°C.

The fitting of the predicted fluxes against those reported in the literature was good in the experiments in which the inlet temperature was varied (Madsen et al., 2019; Motuzas et al., 2018). However, the model was not able to reproduce all the data reported by Madsen et al. (2018), as shown in Figure 4.1 (C). To solve this, two permeabilities were used; a low permeability value,  $k = 2.32\text{E-}16 \text{ m}^2$  allowed to reproduce the experiments with high vacuum pressure (low vacuum level), whereas a high permeability,  $k = 2.82\text{E-}16 \text{ m}^2$ , allowed to fit the experiment at 1.8 kPa. This may imply either that the test at 1.8 kPa was an outlier or that special operational conditions were present during the tests, which could not be reproduced by the model.

Based on the model, it was concluded that the lumen temperature of the solution is a relevant parameter, as it has a direct relationship with the permeate fluxes. From a Darcy's law viewpoint, this occurs because the viscosity of the solution decreases when the temperature rises (Ozbek, 1977) and it favors the permeation at higher velocities. Moreover, a higher temperature increases the vapor pressure of the solution, accelerating the evaporation process on the thin film. In contrast, the vacuum pressure has a



marginal effect in terms of flux, as long as it is below the vapor pressure of the solution at the temperature on the permeate side. This is explained because the pressure gradient  $\nabla p$  in Equation 3.1 is given by the difference of the pressure on the inner side of the membrane (around 101.3 kPa) and the vacuum pressure (between 1.8 and 2.6 kPa). Therefore, the difference in the gradient is negligible, and even an absolute vacuum condition (0 Pa absolute pressure) would not increase  $\nabla p$  significantly. As a final observation derived from the model, the permeabilities of the membranes changed among the different sets of experiments. The lowest permeability  $k$  was observed for the data reported in a solution of 40 g/L of NiSO<sub>4</sub>, while the highest permeabilities were found for ~125 and ~175 g/L NaCl solutions. This suggests a variability in the produced membranes, especially regarding its hydraulic permeability, considering that higher dissolved solids concentrations are related to lower water fluxes (Madsen et al., 2019).

#### **4.2 Obtention and characterization of the industrial ED concentrate**

Kraft pulping effluent, having an initial conductivity of 950  $\mu\text{S}/\text{cm}$ , was electrodialed until reaching a conductivity of 95  $\mu\text{S}/\text{cm}$ , and then replaced

by raw effluent. This step was repeated several times, without purging the reject tank, to obtain at least 1 L of concentrate sample. All removed ions from the treated effluent were transferred into the concentrate tank, and this solution was used for the percrystallization experiments. The characteristics of the feed Kraft effluent and the ED concentrate are shown in Table 4.1.

Table 4.1. Characterization of the Kraft pulping effluent and the concentrate from ED after treatment of the effluent

Parameter	Unit	Feed Kraft effluent	ED Concentrate	Percentage ratio (%TDS)
pH	-	8.02	9.82	--
Conductivity	$\mu\text{s}/\text{cm}$	950	7,910	--
True Color	Pt-Co	16.7	17.7	--
Chemical Oxygen Demand	mg/L	39	53	--
Chloride	mg/L $\text{Cl}^-$	93	900	17.2
Sulphate	mg/L $\text{SO}_4^{2-}$	205	2,192	41.9
Calcium	mg/L Ca	13.0	2.2	0.04
Magnesium	mg/L Mg	1.9	4.2	0.08
Sodium	mg/L Na	260	2,100	40.1
Potassium	mg/L K	9.5	34.0	0.64
Total Dissolved Solids (TDS)	mg/L	582.9	5,233.5	--

Adding up all the measured dissolved species, an approximate value of 5.23 g/L for total dissolved solids is computed. This value is a reference for the quantity of salt contained in the ED concentrate solution. As can be seen from Table 4.1, the main components of the concentrate are sodium, sulphate,

and chloride, representing around 99.2% of the TDS. This is the basis for the synthetic binary solution (BS1 and BS2 of Table 3.2).

### 4.3 Percrystallization performance

The general performance of percrystallization was assessed for different solutions. Pictures of the percrystallization membrane before use and after some tests are shown in Figure 4.2.

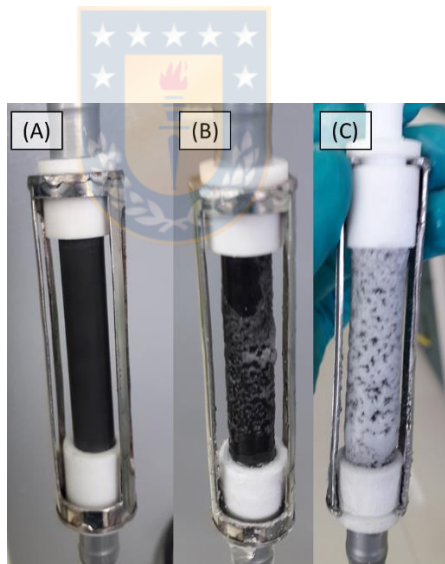


Figure 4.2. Pictures of percrystallization membranes. (A) Pristine hydrophobic membranes, before tests, (B) Salt crust after running the verification test without hotplate, (C) Salt crust after running percrystallization with BS2 solution at 36.5°C.

The crystal observed in Figure 4.2 (B) were found on the external surface of the membrane after the verification test at 36.5°C without the hot plate. No crystals were found in the lumen of the membrane. During this test, some droplets of solution formed on the outer side of the membrane and fell to the bottom of the chamber, which implied that the permeated solution was not evaporating fast enough. A pressure of 30 mbar was measured, indicating that the vacuum pump did not have the sufficient speed to operate at the required low pressures, around 18 mbar according to literature (Madsen et al., 2019; Madsen et al., 2018; Motuzas et al., 2018). Therefore, for the base case with the binary salt and all following tests, the hot plate was included, as was previously shown in Figure 4.2, to aid with the evaporation of the fallen droplets and act as a complementary heat source. Additionally, for the BS1 test, a slightly higher temperature (38°C) was employed to raise the vapor pressure of the solution in a magnitude of around 6 mbar. After these modifications, the percrystallization of the BS1 salts was successfully achieved. The results of the percrystallization experiments (omitting the verification test) are shown in Table 4.2.

Table 4.2. Results of percrystallization experiments

Purpose	Base case		Evaluation		
	BS1	BS2	ED Concentrate		
Removed water (mL)	65	60	120	120	150
Transmembrane flux (L/m <sup>2</sup> /h)	86.6	30.3	60.6	80.8	75.8
Energy consumption (kWh/ton water)	3,723	9,817	4,217	3,217	3,513
Recovered salt (g)	No data	28.8	0.6	0.4	0.4

65 mL of water were evaporated during test with BS1 solution at 38°C, without signs of fouling. However, when operating at a slightly lower temperature (36.5°C) -consequently at a lower water vapor pressure- and for a longer time (BS2 test), a thick crust of crystals was formed on the external surface of the membrane after 60 minutes of operation, as can be seen in Figure 4.2 (C). This explains the reduction of the transmembrane flux and suggest that if the difference between the vacuum and vapor pressure of the solution is not large enough, the evaporation rate diminishes, and the salts have the required time to form crystals on the surface of the membrane. Therefore, although the vacuum pressure is not a relevant parameter in terms of transmembrane flux, it governs the performance of the percrystallization process, especially when it is equal or higher (absolute pressure) than the vapor pressure of the solution (Madsen et al., 2019). The formed crust was easily removed without disturbing the performance of the membrane in subsequent tests. If required, an automatic external cleaning system could be

introduced in industrial applications. It is important to consider that one key advantage of the technology is that the cleaning process would not interrupt the flow of the solution through the interior of the membrane.

No crust was formed on the outer surface of the membrane when working with ED concentrate, even though the tests were carried out at a lower temperature (36.5°C) i.e., a lower vapor pressure, than the unfouled base case (BS1). As the solution had a lower TDS concentration compared to the synthetic solutions used in the other tests, the formation of crystals on the membrane was unlikely and less salt was recovered. Samples of the recovered crystals were analyzed with X-ray diffraction. The diffractogram is shown in Figure 4.3, indicating that the crystals were mainly halite and burkeite, in accordance with the characteristics of the ED concentrate shown in Table 4.1. Although alkalinity was not measured for this sample, in previous experiments with the same effluent, values of around 200 mg/L CaCO<sub>3</sub> were measured, explaining the presence of carbonate in the produced salts.

Measured fluxes were all higher than those reported in literature, around 30 L/m<sup>2</sup>/h (Madsen et al., 2019; Madsen et al., 2018; Motuzas et al., 2018). This may indicate an overestimation of the evaporated water, as it was measured based on the change of feed volume and additional losses may have contributed to this value, such as solution stored inside the pipes that could not be recovered for the after-test volume measurement. On the other hand, the hydrophobic membrane employed in these tests could have a higher permeability (or hydraulic conductivity) than the membranes used in the literature experiments due to differences in the fabrication process. This is supported by the results from the CFD model, which showed that different membranes may have different permeability values  $k$ , probably attributed to differences in the pore size.

Among the percrystallization tests, the lowest energy consumption registered was 2,325 kWh/ton. For all the tests performed with the ED concentrate, energy consumption was well above 3,000 kWh/ton (see Table 4.2). These values are in the same magnitude order as the results of a laboratory scale VMD system, with an energy consumption of 1,100 kWh/ton (Criscuoli, Carnevale, & Drioli, 2008). These high energy consumptions at laboratory

scale are explained because the vacuum pump consumes a large amount of energy but removes only a small mass of water vapor, even though the volumetric vapor flow rate is high, as it has low density due to the low pressure of the system. Considering that traditional ZLD systems, based on evaporators and crystallizers, have consumptions in the order of 90 kWh/ton (Yaqub & Lee, 2019), percrystallization does not come up as an economic alternative for this application based on current laboratory results. However, it is worth to mention that efficiencies at laboratory scale are generally lower than those of an industrial size system. A vacuum pump with a higher flow rate capacity and lower specific energy consumption would be more suitable. Therefore, next section presents energy consumption estimations for an industrial size facility, using a model that better predicts the power consumption of industrial size vacuum pumps.



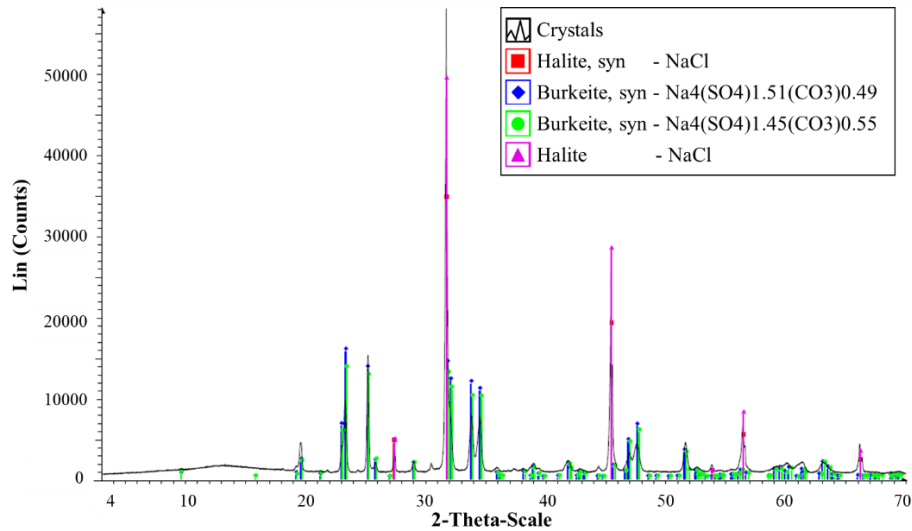


Figure 4.3. Diffractogram of the crystals sample obtained after percrystallization of the ED concentrate

#### 4.4 Energy consumption of an industrial percrystallization system

In an industrial system, the power consumed by the vacuum pumps to maintain low pressures is the main component of the operational expenditures. To decrease the vacuum level and the related power, the temperature of the concentrated effluent can be increased. Under that condition, the required energy to heat the effluent would become increasingly important.

As observed in the previous section, the energy consumption of the vacuum pump and consequently, of the percrystallization system, is considerably higher than those of traditional ZLD systems. However, the employed diaphragm pump was not efficient. Other laboratory scale vacuum pumps could consume less power and deliver a higher air/vapor flow, such as the CC-281 oil pump (JAVAC). Thus, it becomes relevant to use a theoretical and generic model to estimate the specific energy consumption of an optimized system. Calculations described in section 3.6 were used to compute the specific energy consumption of an industrial case (5.4 ton/h of ED concentrate, coming from the treatment of 6,480 m<sup>3</sup>/d of pulping effluent at 30°C, with 98% water recovery by ED), considering an operational temperature range between 37°C and 90°C. The results are shown in Figure 4.4.

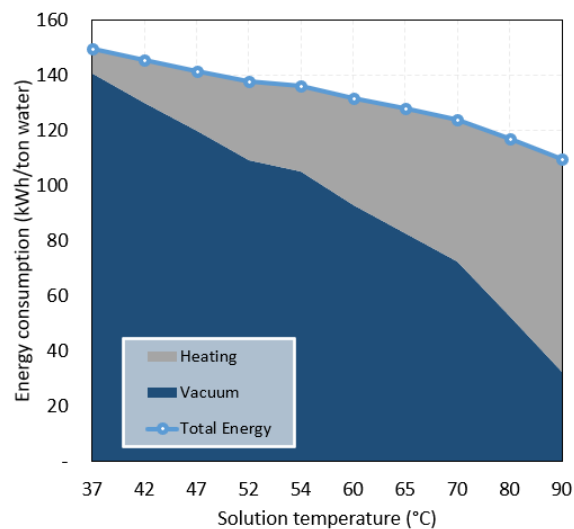


Figure 4.4. Specific energy consumption of an industrial percrystallization system depending on the temperature of the solution in the lumen of the membranes. The raw ED concentrate has a temperature of 30°C.

As expected, by increasing the temperature of the solution less vacuum is needed to achieve percrystallization. The density of vapor at higher pressures rises and consequently, the work of the vacuum pump becomes more efficient, having a lower energy consumption per ton of evaporated water. The energy required to heat the solution increases with temperature, but the overall consumption of the system diminishes, from 150 kWh/ton at 37°C to 110 kWh/ton at 90°C feed solution temperature.

The theoretical industrial energy consumptions of a percrystallization system are an order of magnitude lower than those measured in our experiments, in a similar way to how the energy of a VMD system would decrease from 1,100 kWh/ton at laboratory scale (Criscuoli et al., 2008) to 699 kWh/ton in an industrial size facility (Miladi et al., 2021). Based on performed calculations, which omit auxiliary equipment power, percrystallization seems to be a more efficient alternative than VMD. However, these values are still higher than those of traditional ZLD systems such as MVCs, suggesting that percrystallization may not be a suitable technology for ZLD processes, mainly because of to the large amounts of energy consumed by vacuum pumps to remove high volumes of vapor produced by small quantities (mass) of evaporated water, due to the low density of vapor at the working chamber pressure. Operation at higher temperatures and vapor pressures is more efficient, as seen in Figure 4.4, but the additional energy required to heat the solution makes the overall consumption higher than the goal of 90 kWh/ton of traditional ZLD systems. Nevertheless, if the heating energy was obtained from low-cost sources such as solar thermal energy, percrystallization might become a preferred option over MVCs, especially considering that crystals

are separated from water in a single step, without the need of filters or centrifuges.

One additional challenge related with the technology, considering its current maturity, is the large-scale production of membranes to allow continuous evaporation of the concentrated solution. For the evaluated industrial case, considering the average of the transmembrane fluxes during the tests with the ED concentrate (see Table 4.2), an area of 74.6 m<sup>2</sup> would be required to treat the incoming concentrate at a flowrate of 5.4 ton/h. Supposing long membranes (1 m length, 1 cm external diameter), around 2,375 membranes would be needed in this specific case. The fluxes and required area are in the same magnitude order as those found in nanofiltration, between 10 and 42 L/m<sup>2</sup>/h (Andrade, Aguiar, Pires, Grossi, & Amaral, 2017), and reverse osmosis, between 19 and 28 L/m<sup>2</sup>/h (Lee, Arnot, & Mattia, 2011).

Another application different than ZLD would be the production of valuable crystals that only form in a low-medium temperature range, as the vacuum driven percrystallization process allows evaporation at low temperatures (Bharmoria, Gehlot, Gupta, & Kumar, 2014; Wu, 2020).

## CHAPTER 5: CONCLUSIONS

The percrystallization technique was evaluated as a core technology for industrial zero liquid discharge applications. For this, a CFD model was first applied as a tool to better understand the critical parameters of percrystallization and the physical phenomena that occur in the process. It was determined that feed water temperature is a critical parameter to adjust, as it controls the viscosity of the solution and, subsequently, its permeation through the membrane (as explained by Darcy's law), whereas vacuum pressure is not as critical as expected to improve transmembrane flux. However, vacuum pressure must be sufficiently lower than the water vapor pressure to allow evaporation of the permeated solution.

Experimental analyses were performed using simple and binary salt solutions, the former to verify that the technique is reproducible, compared with literature experiences, and the latter to include the main components of a Kraft pulping effluent. Thirdly, a real industrial effluent was concentrated with electrodialysis to be subsequently treated by percrystallization, successfully achieving percrystallization in all cases. However, a high energy

consumption was obtained at laboratory scale, mainly because of the type of vacuum pump employed and non-optimized conditions of percrystallization. Finally, to evaluate percrystallization electrical costs at full-scale, theoretical calculations were used to project the energy consumption of an industrial percrystallization system, considering industrial vacuum pumps. Although the operational cost is reduced 10 times compared with laboratory trials, it is still above conventional ZLD technologies. Contrary to preliminary assumptions, percrystallization consumes more energy than traditional evaporation systems and is not an efficient alternative for ZLD in the pulp industry, considering the high flow rates that must be evaporated and the temperature of the effluent (around 30°C). Nevertheless, percrystallization could still be convenient at small-medium scale or with labile samples that must be dried at low temperatures to avoid altering its characteristics. New research on this topic should focus on this line of work. In parallel, the development of more efficient vacuum systems could help to turn percrystallization into an attractive alternative for industrial ZLD.

## REFERENCES

- Ali, A., Quist-Jensen, C. A., Macedonio, F., & Drioli, E. (2015). Application of Membrane Crystallization for Minerals' Recovery from Produced Water. *Membranes (Basel)*, 5(4), 772-792. doi:10.3390/membranes5040772
- Andrade, L. H., Aguiar, A. O., Pires, W. L., Grossi, L. B., & Amaral, M. C. S. (2017). Comprehensive bench- and pilot-scale investigation of NF for gold mining effluent treatment: Membrane performance and fouling control strategies. *Separation and Purification Technology*, 174, 44-56. doi:10.1016/j.seppur.2016.09.048
- Bharmoria, P., Gehlot, P. S., Gupta, H., & Kumar, A. (2014). Temperature-dependent solubility transition of Na<sub>2</sub>SO<sub>4</sub> in water and the effect of NaCl therein: solution structures and salt water dynamics. *J Phys Chem B*, 118(44), 12734-12742. doi:10.1021/jp507949h
- Chabanon, E., Mangin, D., & Charcosset, C. (2016). Membranes and crystallization processes: State of the art and prospects. *Journal of Membrane Science*, 509, 57-67. doi:10.1016/j.memsci.2016.02.051
- Chen, Q.-B., Ren, H., Tian, Z., Sun, L., & Wang, J. (2019). Conversion and pre-concentration of SWRO reject brine into high solubility liquid salts (HLS) by using electrodialysis metathesis. *Separation and Purification Technology*, 213, 587-598. doi:10.1016/j.seppur.2018.12.018
- COMSOL. (2005). COMSOL Multiphysics (Version V 4.4). <https://www.comsol.com/>: COMSOL Inc. Retrieved from <https://www.comsol.com/>
- Criscuoli, A., Carnevale, M. C., & Drioli, E. (2008). Evaluation of energy requirements in membrane distillation. *Chemical Engineering and Processing: Process Intensification*, 47(7), 1098-1105. doi:10.1016/j.cep.2007.03.006



- Drioli, E., Di Profio, G., & Curcio, E. (2012). Progress in membrane crystallization. *Current Opinion in Chemical Engineering*, 1(2), 178-182. doi:10.1016/j.coche.2012.03.005
- Elimelech, M., & Phillip, W. A. (2011). The Future of Seawater Desalination: Energy, Technology, and the Environment. *Science*, 333(6043), 712-717. doi:10.1126/science.1200488
- Evans, T. (1995). Applying proven technology to eliminate kraft bleach plant effluents. *Pulp & Paper Canada*, 96(3), 60-64. Retrieved from <https://search.proquest.com/docview/232779356?accountid=15690>
- Gonzalez-Vogel, A., Moltedo, J. J., Reyes, R. Q., Schwarz, A., & Rojas, O. J. (2021). High frequency pulsed electro dialysis of acidic filtrate in kraft pulping. *J Environ Manage*, 282, 111891. doi:10.1016/j.jenvman.2020.111891
- Havelka, J., Farova, H., Jiricek, T., Kotala, T., & Kroupa, J. (2019). Electro dialysis-based zero liquid discharge in industrial wastewater treatment. *Water Sci Technol*, 79(8), 1580-1586. doi:10.2166/wst.2019.161
- Heijman, S. G. J., Guo, H., Li, S., van Dijk, J. C., & Wessels, L. P. (2009). Zero liquid discharge: Heading for 99% recovery in nanofiltration and reverse osmosis. *Desalination*, 236(1-3), 357-362. doi:10.1016/j.desal.2007.10.087
- Huang, J. (2018). A Simple Accurate Formula for Calculating Saturation Vapor Pressure of Water and Ice. *Journal of Applied Meteorology and Climatology*, 57(6), 1265-1272. doi:10.1175/jamc-d-17-0334.1
- Klein, E., Ward, R. A., & Lacey, R. E. (1987). Membrane Processes- Dialysis and Electro dialysis. In R. W. Rousseau (Ed.), *Handbook of Separation Process Technology*. Georgia: John Wiley & Sons.
- Lee, K. P., Arnot, T. C., & Mattia, D. (2011). A review of reverse osmosis membrane materials for desalination—Development to date and future potential. *Journal of Membrane Science*, 370(1-2), 1-22. doi:10.1016/j.memsci.2010.12.036

- Madsen, R. S. K., Motuzas, J., Julbe, A., Vaughan, J., & Diniz da Costa, J. C. (2019). Novel membrane percrystallisation process for nickel sulphate production. *Hydrometallurgy*, 185, 210-217. doi:10.1016/j.hydromet.2019.02.015
- Madsen, R. S. K., Motuzas, J., Vaughan, J., Julbe, A., & Diniz da Costa, J. C. (2018). Fine control of NaCl crystal size and particle size in percrystallisation by tuning the morphology of carbonised sucrose membranes. *Journal of Membrane Science*, 567, 157-165. doi:10.1016/j.memsci.2018.09.003
- McGinnis, R. L., Hancock, N. T., Nowosielski-Slepowron, M. S., & McGurgan, G. D. (2013). Pilot demonstration of the NH<sub>3</sub>/CO<sub>2</sub> forward osmosis desalination process on high salinity brines. *Desalination*, 312, 67-74. doi:10.1016/j.desal.2012.11.032
- Mickley, M. (2008). *Survey of High-Recovery and Zero Liquid Discharge Technologies for Water Utilities*. Retrieved from WateReuse Foundation:
- Miladi, R., Frikha, N., & Gabsi, S. (2021). Modeling and energy analysis of a solar thermal vacuum membrane distillation coupled with a liquid ring vacuum pump. *Renewable Energy*, 164, 1395-1407. doi:10.1016/j.renene.2020.10.136
- Motuzas, J., Yacou, C., Madsen, R. S. K., Fu, W., Wang, D. K., Julbe, A., . . . Diniz da Costa, J. C. (2018). Novel inorganic membrane for the percrystallization of mineral, food and pharmaceutical compounds. *Journal of Membrane Science*, 550, 407-415. doi:10.1016/j.memsci.2017.12.077
- Nayar, K. G., Fernandes, J., McGovern, R. K., Al-Anzi, B. S., & Lienhard, J. H. (2019). Cost and energy needs of RO-ED-crystallizer systems for zero brine discharge seawater desalination. *Desalination*, 457, 115-132. doi:10.1016/j.desal.2019.01.015
- Oasys Water, I. (2017). Changxing Power Plant Debuts The World's First Forward Osmosis-Based Zero Liquid Discharge Application. Retrieved from <https://www.wateronline.com/doc/changxing-power->

[plant-debuts-the-world-s-first-forward-osmosis-based-zero-liquid-discharge-application-0001](#)

- Oren, Y., Korngold, E., Daltrophe, N., Messalem, R., Volkman, Y., Aronov, L., . . . Gilron, J. (2010). Pilot studies on high recovery BWRO-EDR for near zero liquid discharge approach. *Desalination*, 261(3), 321-330. doi:10.1016/j.desal.2010.06.010
- Ozbek, H. (1977). *Viscosity of Aqueous Sodium Chloride Solutions from 0 - 150°C*. Retrieved from American Chemical Society 29th Southeast Regional Meeting, Tampa, FL.: <https://escholarship.org/uc/item/3jp6n2bf>
- Plawsky, J. L., Fedorov, A. G., Garimella, S. V., Ma, H. B., Maroo, S. C., Chen, L., & Nam, Y. (2014). Nano- and Microstructures for Thin-Film Evaporation—A Review. *Nanoscale and Microscale Thermophysical Engineering*, 18(3), 251-269. doi:10.1080/15567265.2013.878419
- Pramanik, B. K., Thangavadiel, K., Shu, L., & Jegatheesan, V. (2016). A critical review of membrane crystallization for the purification of water and recovery of minerals. *Reviews in Environmental Science and Bio/Technology*, 15(3), 411-439. doi:10.1007/s11157-016-9403-0
- Ranjan, R., Murthy, J. Y., & Garimella, S. V. (2011). A microscale model for thin-film evaporation in capillary wick structures. *International Journal of Heat and Mass Transfer*, 54(1-3), 169-179. doi:10.1016/j.ijheatmasstransfer.2010.09.037
- Ruiz Salmón, I., & Luis, P. (2018). Membrane crystallization via membrane distillation. *Chemical Engineering and Processing - Process Intensification*, 123, 258-271. doi:10.1016/j.cep.2017.11.017
- Tong, T., & Elimelech, M. (2016). The Global Rise of Zero Liquid Discharge for Wastewater Management: Drivers, Technologies, and Future Directions. *Environ Sci Technol*, 50(13), 6846-6855. doi:10.1021/acs.est.6b01000
- Valladares Linares, R., Li, Z., Sarp, S., Bucs, S. S., Amy, G., & Vrouwenvelder, J. S. (2014). Forward osmosis niches in seawater

desalination and wastewater reuse. *Water Res*, 66, 122-139. doi:10.1016/j.watres.2014.08.021

- Wu, H. (2020). *Effect of sodium chloride on the formation of ice and salt during eutectic freeze crystallization of sodium sulfate with a scenario study of real brine*. (Master of Science in Civil Engineering, Track of Environmental Engineering). Delft University of Technology, Retrieved from <https://repository.tudelft.nl/islandora/object/uuid%3Ac2fe085c-429f-48b1-bbab-d6b0ea19cbbf>
- Xiao, R., Maroo, S. C., & Wang, E. N. (2013). Negative pressures in nanoporous membranes for thin film evaporation. *Applied Physics Letters*, 102(12). doi:10.1063/1.4798243
- Yaqub, M., & Lee, W. (2019). Zero-liquid discharge (ZLD) technology for resource recovery from wastewater: A review. *Sci Total Environ*, 681, 551-563. doi:10.1016/j.scitotenv.2019.05.062
- Zhao, D., Lee, L. Y., Ong, S. L., Chowdhury, P., Siah, K. B., & Ng, H. Y. (2019). Electrodialysis reversal for industrial reverse osmosis brine treatment. *Separation and Purification Technology*, 213, 339-347. doi:10.1016/j.seppur.2018.12.056
- Zhao, J.-J., Duan, Y.-Y., Wang, X.-D., & Wang, B.-X. (2011). Effect of nanofluids on thin film evaporation in microchannels. *Journal of Nanoparticle Research*, 13(10), 5033-5047. doi:10.1007/s11051-011-0484-y